

## A preliminary analysis of solid-gas flows and buoyant convection through solar receivers

Kuruneru, S.T.W.<sup>1</sup>, Kim, J.S.<sup>1</sup>, Soo Too, Y.<sup>1</sup>

<sup>1</sup>*The Commonwealth Scientific & Industrial Research Organization, NSW 2304, Australia*

### Introduction

Concentrated solar power (CSP) would potentially play an important role in meeting world energy demand [1-2]. Particle receivers for CSPs are an attractive alternative to traditional receivers using molten salts or nanofluids as the heat transfer fluids (HTFs). Solid spherical particles such as ceramic are non-toxic, easy to handle, inexpensive, chemically stable, and able to withstand high flux and temperature [2]. A lot of research was conducted on particle receiver technology for CSP plants, such as free-falling particle receivers. However, a thorough fundamental analysis of the solid-gas flows and quantifying heat losses through solar particle receivers are still lacking. The scarcity of these studies stems from the fact that the heat losses are extremely difficult, if not impossible, to quantify using experimental methods. A workaround is to develop advanced numerical models with the goal of quantifying heat losses through receiver aperture, which would ultimately provide useful information for engineers and scientists to better optimize CSP particle receiver designs.

### Development of Numerical Model

In this study, a coupled computational fluid dynamics and discrete particle method (CFD-DPM) is developed in an open-source program, OpenFOAM with the goal of quantifying heat losses. The entire mathematical formulation of the CFD-DPM is found in [3-4]. In this study, the particle-particle interactions/collisions are neglected because the particles rapidly accelerate towards the bottom of the cavity receiver and due to the high solid-gas density ratio considered in this study, the particle-particle interactions are negligible. Hence, DPM is used instead of DEM (Discrete Element Method). The solid-gas density ratio is  $\gg 1$ , so the solid-gas hydrodynamic forces considered are gravity and drag. The Ranz-Marshall correlation is deployed to account for convective heat transfer between solid-gas phase. For brevity, radiation models are not deployed. The kOmegaSST turbulence model is deployed and temperature dependent fluid properties is enforced due to the high Reynolds numbers and operating temperatures considered in this study. The Pressure Implicit Splitting of Operators (PISO) is deployed for the pressure-velocity coupling ( $n_{\text{OuterCorrectors}} = 1$ ;  $n_{\text{NonOrthogonalCorrectors}} = 1$ ;  $n_{\text{Correctors}} = 2$ ). Various discretization schemes are used such as Euler (time), Gauss Linear (gradient), Gauss Upwind (divergence), Gauss linear uncorrected (Laplacian), Linear (interpolation), uncorrected (surface normal gradient), meshWave (to calculate distance of cell centres and boundary, which is required for turbulence model). Also, the preconditioned conjugate gradient (PCG), preconditioned bi-conjugate gradient stabilized (PBiCGStab) solvers and also the Diagonal-based Incomplete Cholesky (DIC) and the Simplified Diagonal-based Incomplete LU (DILU) preconditioners are used to solve for the discretized equations of momentum and energy. The residuals are set to  $10^{-5}$  and  $10^{-7}$  for , respectively. The time-step is set to  $10^{-5}$ s and the maximum Courant number is set to 1 with adjustable time step enabled from  $10^{-4}$ s and  $10^{-5}$ s. The interpolation schemes for the lagrangian (DPM) are deployed, namely *cell* interpolation (assumes values are constant through a CFD cell) which interpolates between a DPM particle's position/velocity/temperature and the CFD mesh cell where the DPM particle is located. Maximum particle Courant number is set to 0.3. The *cell* interpolation is used for density, energy, etc., whereas the *cellPoint* interpolation (linear weighted interpolation) is used for velocity. The Euler intergration scheme is used for integration of DPM velocity and analytical integration for DPM temperature. For coupled simulations, explicit schemes are deployed for the treatment of source terms in the momentum and energy equations of continuous phase (*i.e.* explicit momentum and energy source for DPM particles). The coupled CFD-DPM is developed specifically to calculate the momentum and energy exchange between the solid ceramic particles, the

surrounding fluid, and the receiver walls. The finite volume method is used to solve for the continuum fluid phase, and the discrete particle method is used to solve for the lagrangian solid phase. The geometry and boundary conditions of the receiver is shown in Figure 1. The geometry is designed in SolidWorks and the computational mesh is created in cfMesh. A velocity inlet (Inlet1) is assigned to one end of the enclosure with a head-on wind velocity of 0.5 m/s, and all other sides of the rectangular enclosure is exposed to the ambient air. The receiver also has a 0.1m × 0.1m square opening (aperture) which allows fluid to flow into/out of this aperture. The entry length (distance from Inlet1 to the Receiver aperture) is set to 10 times the size of the receiver aperture (0.1m). To prevent numerical instability and spurious data, the DPM particles are injected via Inlet 2 at 10 s. A closer view of the cavity receiver is shown as well. The solid particles with an initial velocity of 0.25 m/s, at a rate of 100,000 particles per second, are injected into the cavity through Inlet2, and the particles can settle towards Outlet2 under the action of gravity. Conjugate heat transfer of fluid through the wall is not modelled. Instead, all outer walls are assumed to be adiabatic and inner walls are set to specific wall temperature, as shown in Figure 1. The solid spherical particles are based on ceramic proppant with a diameter and density of 350 μm and 3600 kg/m<sup>3</sup>, respectively. The solid particles are assumed smooth, spherical, and cohesionless. The cooling (heat dissipation) of the solid particles to the fluid is not considered, hence the specific heat capacity of the solid particles is set to 100 times greater than the actual specific heat capacity (1275 J/(kg K)) of ceramic particles. This is done to keep the temperature of the entire particle temperature constant at 800°C.

## Results

The solid-gas temperature and velocity characteristics of a small section of the domain are shown in Figure 2. It is noted that the particle curtain is continuously being injected along the Inlet2 plane, and as time elapses, the curtain settles towards Outlet2 (bottom of the heated cavity) under the action of gravity. The incoming head-on wind from Inlet1 flows into the cavity through the receiver's aperture and the fluid temperature gradually increases due to the heated particle curtain, which heats the surrounding fluid due to solid-gas convection. As the fluid heats up, the fluid located further away from the particle curtain traverses towards the top of the cavity and leaves the aperture due to the buoyant convection effects. Additionally, as the particle curtain settles towards Outlet2, the fluid around the immediate vicinity of the particle curtain also traverses towards Outlet2 because of the drag effects of the particle curtain. As such the presence of the particle curtain leads to two distinct fluid flow profiles denoted by the fluid velocity vectors. It is noted that the fluid velocity leaving the cavity (near the top aperture lip) is slightly higher than the velocity of the incoming fluid (into the cavity). The heat flowing into and out of the receiver is, respectively, -473W and +831W. The heat flowing through Inlet2 and Outlet2 is, respectively, -18W and +125W. The total/net heat is 465W and the heat losses through the aperture is 404W ( $465W \times \frac{831W}{125W+831W}$ ).

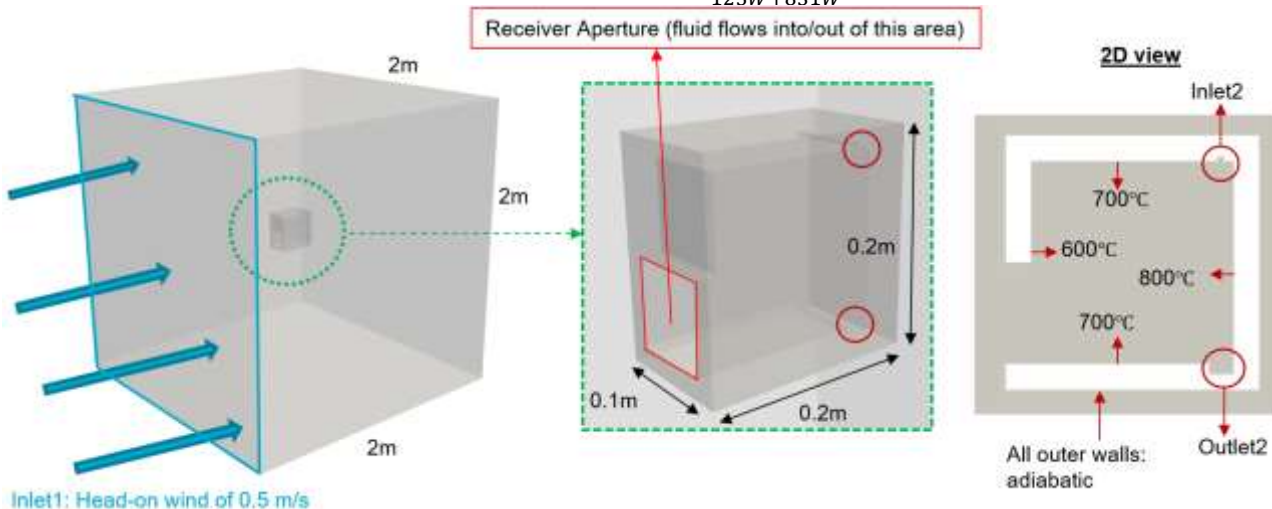
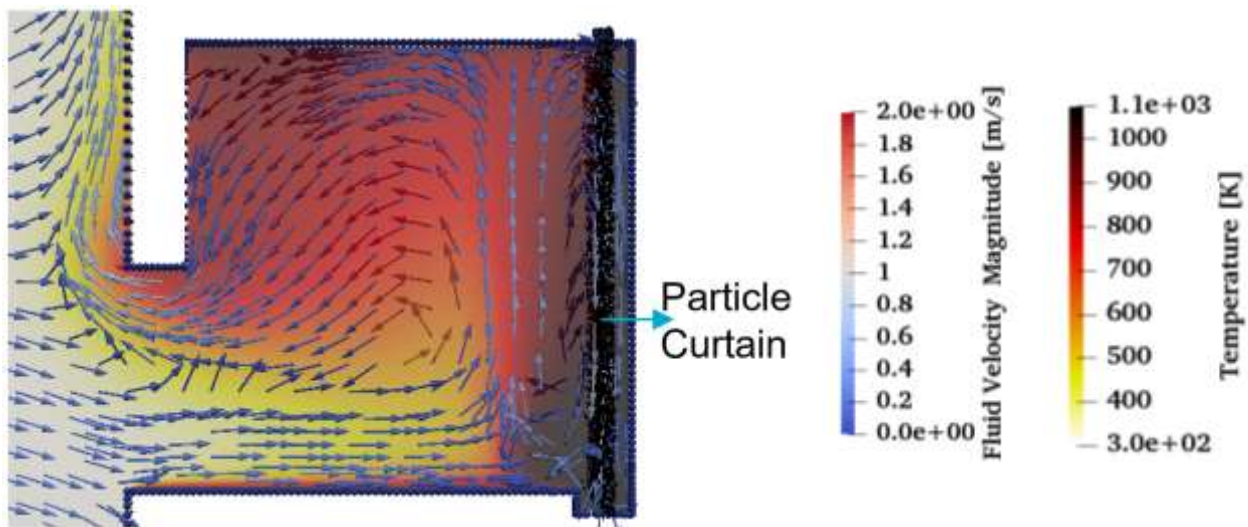


Figure 1. Computational domain of cavity receiver.



**Figure 2. Close-up view of buoyant convection of solid-gas flows taken at 60 s. Note that the particle curtain is denoted by the dotted region.**

The amount of heat leaving the aperture is due to the buoyant convection effects. The heated particle curtain and the geometrical morphology of the cavity receiver has profound implications on the heat fluxes through the receiver aperture, which is denoted by the different fluid velocity patterns in the cavity receiver. The next step is to assess heat losses based on different particle flow rates, inlet velocity conditions and various geometries.

## Conclusions

A coupled CFD-DPM is developed and implemented in OpenFOAM to assess solid-gas thermal characteristics and quantify heat fluxes through CSP receivers. The fluid around the immediate vicinity of the particle curtain traverses towards Outlet2 due to the drag effects of the heated particle curtain. Also, the fluid located away from the particle curtain steadily flows towards the top of the receiver before leaving the aperture due to buoyant convection effects. Additional research is currently in progress, which includes conducting a comparative analysis of heat losses (through receiver aperture) based various particle flow rates, inlet velocity conditions, and various geometries.

## Acknowledgements

This research was funded by the Australian Solar Thermal Research Institute (ASTRI), which is supported by the Australian Government, through the Australian Renewable Energy Agency.

## References

- [1] Huang, Y, 2014, Drivers of rising global energy demand: The importance of spatial lag and error dependence, *Energy*, 76, p254-263.
- [2] Ho, C., and Iverson, B, 2014, Review of High-Temperature Central Receiver Designs for Concentrating Solar Power, *Renewable Sustainable Energy Review*, 29, p835-846.
- [3] Kuruneru, S.,...,Gu, Y, 2019, A comparative study of mixed resolved-unresolved CFD-DEM and unresolved CFD-DEM methods for the solution of particle-laden liquid flows, *Archives of Computational Methods in Engineering*, 26, p1239-1254.
- [4] Norouzi, H.,...,Mostoufi, N, 2016, *Coupled CFD-DEM Modeling : Formulation, Implementation and Application to Multiphase Flows (1st ed.)*. Wiley.